Inorganic Chemistry, Vol. 14, No. 4, 1975 **767**

Contribution from the Chemistry Department,
University of Virginia, Charlottesville, Virginia 22901

Infrared and Raman Studies of Alkali Metal–Chlorine Reaction Products. Resonance Raman Spectrum of the Chlorine Molecular Anion, Cl_2^-

WILMONT F. HOWARD, Jr. and LESTER ANDREWS*

Received August 9, 1974 AIC40558U

The products of alkali metal atom matrix reactions with molecular chlorine have been examined by laser Raman and infrared spectroscopy. The yellowish orange $M^+Cl_2^-$ species produced resonance Raman spectra using 4579–5145-Å excitation; extensive progressions up to 9ν of Cl_2^- were observed. The calculated harmonic and anharmonic vibrational constants yielded values for the Cl_2^- dissociation energy in excellent agreement with the thermodynamic value.

Introduction

Recent success with fluorine–alkali metal reactions, producing the $M^+F_2^-$ species,[1] suggested a search for the chlorine anion, Cl_2^-, in a similar fashion. γ irradiation of crystalline chloride salts produced V centers which have been studied by electron spin resonance and attributed to Cl_2^-.[2] Hass and Griscom[3] have attributed a Raman band at 265 cm^{-1} in γ-irradiated alkali halide–alkali borate glasses to the Cl_2^- fundamental. Person[4] has estimated properties of the chlorine molecular anion, and Minturn, *et al.*,[5] have proposed an $M^+Cl_2^-$ intermediate in crossed molecular beam reactions.

This study was pursued using both infrared and Raman spectroscopy, although only the two lightest alkali metals were employed in the infrared work due to instrumental low-frequency limitations. The former provided a contrast with gas-phase and matrix-isolated alkali chloride frequencies and yielded a direct route to the production and spectral characterization of alkali chloride dimers and higher aggregates, previously obtained only by Knudsen cell–salt effusion matrix experiments.[6,7] The latter gave resonance Raman spectra for the yellowish orange $M^+Cl_2^-$ species using blue argon ion laser exciting lines, which has been communicated earlier.[8] The resonance Raman vibrational progressions yielded the harmonic and first-order anharmonic vibrational frequencies (ω_e and $\omega_e x_e$, respectively), as well as an upper limit of the dissociation energy of the species under examination, which may be used as a check on thermodynamically obtained measurements. The resonance Raman effect may also serve to outline an absorption profile of the reaction product molecular species.

Experimental Section

The same apparatus described in the previous paper[1] was used for the chlorine–alkali metal atom reaction studies.

Chlorine (Matheson) was condensed in a finger with liquid nitrogen and outgassed to remove any volatile impurities. $^{37}Cl_2$ was prepared by oxidizing $Rb^{37}Cl$ in concentrated HNO_3; the effluent gas was passed through Drierite, condensed, and outgassed. Argon (Air Products, 99.995%) and chlorine matrix samples were prepared in the stainless steel vacuum system using standard techniques. In several experiments, krypton and xenon (Matheson, research grade) matrix gases were used.

The experimental run procedure and spectroscopy were performed as reported in the previous study.[1] Reported frequency measurements are accurate to ±0.5 cm^{-1} or the rms deviation of several measurements from the average.

Results

All the experiments comprising this study were run at a matrix:Cl_2 ratio of 100:1. A Raman blank (no metal) of matrix-trapped Cl_2 revealed a partially resolved triplet at 538.6, 531.0, and 523.2 ± 1.0 cm^{-1}, while regions appropriate to the alkali chloride vibrational frequencies were void of signals in metal-added Raman experiments. Matrices containing the alkali metal–chlorine intermediates appeared yellowish orange in white light which served as an effective monitor of the reaction. Results corresponding to each alkali metal will be treated separately, and Figure 1 highlights the Raman spectra of various alkali metal–chlorine intermediates in the region 200–600 cm^{-1}.

Table I. Observed and Calculated Frequencies in the Resonance Raman Progressions of $Li^+(^{35}Cl_2)^-$ and $Li^+(^{35}Cl^{37}Cl)^-$

Vibrational quantum no.	$Li^+(^{35}Cl_2)^-$ freq, cm^{-1}		$Li^+(^{35}Cl^{37}Cl)^-$ freq, cm^{-1}	
	Obsd	Calcd	Obsd	Calcd
1	245.9 ± 0.8	245.9		242.9
2	488.3 ± 0.8	488.5	483.0 ± 0.6	482.8
3	728.1 ± 0.9	727.9	719.4 ± 0.6	719.6
4	963.6 ± 0.7	964.1	952.5 ± 0.7	953.4
5	1198.0 ± 0.8	1197.1	1184.7 ± 0.7	1184.1
6	1427.5 ± 1.2	1426.8		1411.7
7	1652.5 ± 1.0	1653.4	1637.5 ± 1.0	1636.2
8	1876.3 ± 1.0	1876.7		1857.7
9	2096.9 ± 0.8	2096.7	2075.1 ± 1.0	2076.1

Lithium. The Raman spectra of solid Ar-trapped Li–Cl_2 reaction products have been reported earlier.[8] The calibrated frequency shifts for the progression members are listed in Table I. This regularly decreasing intensity pattern, with a 245.9 ± 0.5 cm^{-1} fundamental, eight overtones, and lower frequency-shifted partners with six of the overtone signals, was created with 5145- and 4880-Å excitation; higher energy Ar^+ laser lines (4765 and 4579 Å) yielded shorter series. Lithium isotopic substitution made no discernible changes in the Raman spectra, while a weak band at 273 ± 2 cm^{-1} was noted in most of the Li experiments. A Xe–Cl_2 trial with ^7Li yielded a Raman spectrum with a well-defined triplet at 540.4, 533.0, and 525.6 ± 1.0 cm^{-1} and included a very strong band at 243.0 ± 0.7 cm^{-1}, with weak features at 253.4 ± 0.7 and 484.7 ± 0.6 cm^{-1}. An Ar–$^{37}Cl_2$ (99% enriched) experiment with lithium showed four bands in the Raman scan: a series at 241.4 ± 0.5, 476.5 ± 0.9, and 707.8 ± 1.0 cm^{-1} and a lone band at 522.1 ± 0.5 cm^{-1}.

The infrared spectra of matrix-trapped ^6Li and ^7Li–Cl_2 reaction products are shown in Figure 2; the spectrum from a mixed isotopic run (^6Li:^7Li = 1) was not included. The strongest signal in the ^6Li trial, found at 616.9 cm^{-1} (0.35) (optical densities are given parenthetically), was subsequently lowered to 579.5 cm^{-1} (0.44) with ^7Li; both bands were asymmetric to lower frequency. A moderately intense band at 552.4 cm^{-1} (0.10) with ^6Li reappeared at 517.8 cm^{-1} (0.13) in the ^7Li examination, while a triplet observed at 519.6 (0.14), 511.4 (0.22), and 501.3 cm^{-1} (0.17) in ^6Li runs shifted to 489.2 (0.13), 481.1 (0.19), and 469.6 cm^{-1} (0.21) with the heavier isotope. Lastly, ^6Li experiments revealed a moderately intense band at 375.7 cm^{-1} (0.21) and a weak signal at 312.8 cm^{-1} (0.05), which were found at 352.6 (0.18) and 297.0 (0.05) cm^{-1}, respectively, using ^7Li.

The $^{6,7}Li$ experiment recreated the bands listed above, but at reduced intensities. An additional feature at 491.3 cm^{-1} (0.12) was noted, and a 1:2:1 triplet was calibrated at 375.5

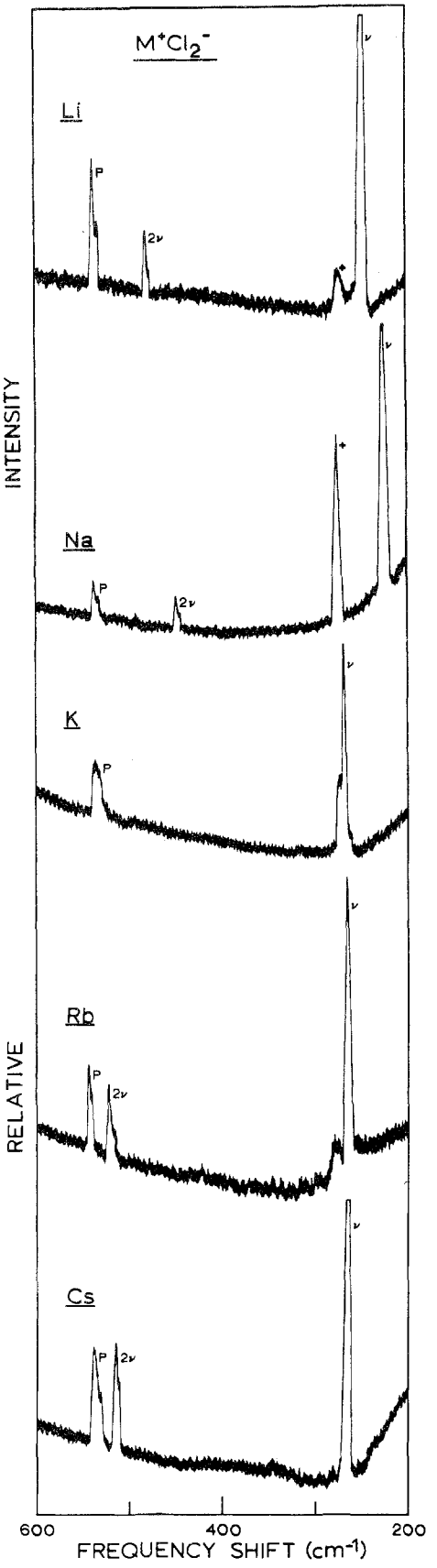

Figure 1. Matrix Raman spectra of alkali metal–chlorine reaction products in the region 200–600 cm^{-1}. P is the Cl_2 signal, ν and 2ν are attributed to the Cl–Cl stretch in $M^+Cl_2^-$ species, and + may be ν_1 of Cl_3^- in $M^+Cl_3^-$ (see text). Instrumental parameters: all scans in the 0.3×10^{-9} A range, 3-sec rise time; 20-cm^{-1}/min scan speed, 5-Å dielectric filter, Li, Na, K–150 mW of 4880-Å excitation, Rb–75 mW of 4765-Å excitation, Cs–60 mW of 4579-Å excitation (12-Å filter).

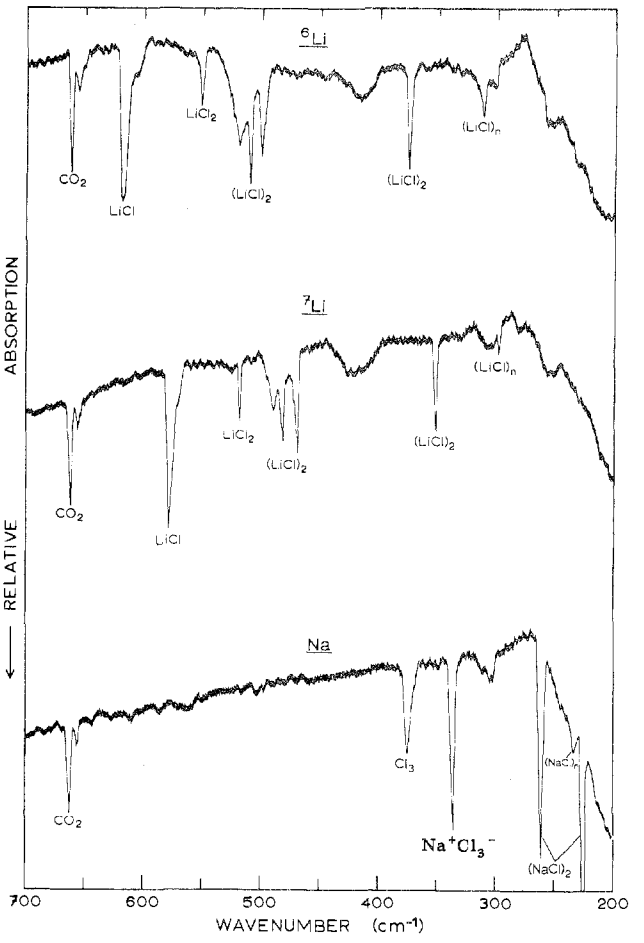

Figure 2. Infrared spectra of chlorine and isotopic lithium or sodium matrix reaction products. Instrumental parameters: 40-cm^{-1}/min scan speed; 5% gain. Band assignments are shown on spectra.

(0.09), 362.4 (0.17), and 352.5 cm^{-1} (0.08). The signals between 510 and 520 cm^{-1} in ^6Li trials appeared merged into a single broad band with no distinct components. No additional band was observed between 520 and 550 cm^{-1}.

Sodium. The most intense signal in Ar-matrix Raman spectra of Na–Cl_2 reaction products was found at 224.9 ± 0.5 cm^{-1}, with a weak overtone at 447.6 ± 0.7 cm^{-1}. A moderately strong band at 274.0 ± 1.0 cm^{-1} was calibrated, and the molecular Cl_2 feature at 538 and 530 cm^{-1} was found to have about the same intensity (60% of the 225-cm^{-1} signal). A Xe–Cl_2 experiment was conducted with Na; besides the Cl_2 triplet at 540–520 cm^{-1}, a strong band was noted at 219.1 ± 0.8 cm^{-1} and weaker signals at 254.6 ± 0.9 and 276.0 ± 0.8 cm^{-1}. An identical trial with Kr diluent yielded the 273-cm^{-1} band 5 times as strong as the 225 cm^{-1} feature, while the Cl_2 signal was observed at 539.4 ± 0.8 and 531.8 ± 1.0 cm^{-1}.

An infrared survey scan of the Ar–Cl_2 with Na system is included in Figure 2. Other than the CO_2 impurity doublet, there was an asymmetric band at 374 cm^{-1} (0.22), a strong signal at 335.8 cm^{-1} (0.50), two very strong features at 272.0 (0.76) and 225.5 cm^{-1} (completely absorbing), and a weak member at 234 cm^{-1} (0.20).

Potassium. The strongest feature in the K–Cl_2 Raman spectra was found at 264.1 ± 0.5 cm^{-1}, accompanied by a shoulder at 271.6 ± 0.8 cm^{-1}. A possible overtone from this intense band would be coincident with the Cl_2 fundamental, and if this overtone was present, it was swamped by the Cl_2 signal. A search for the third member of the progression was unsuccessful with all of the Ar^+ laser lines.

Rubidium. Laser excitation with 4880-Å light yielded a

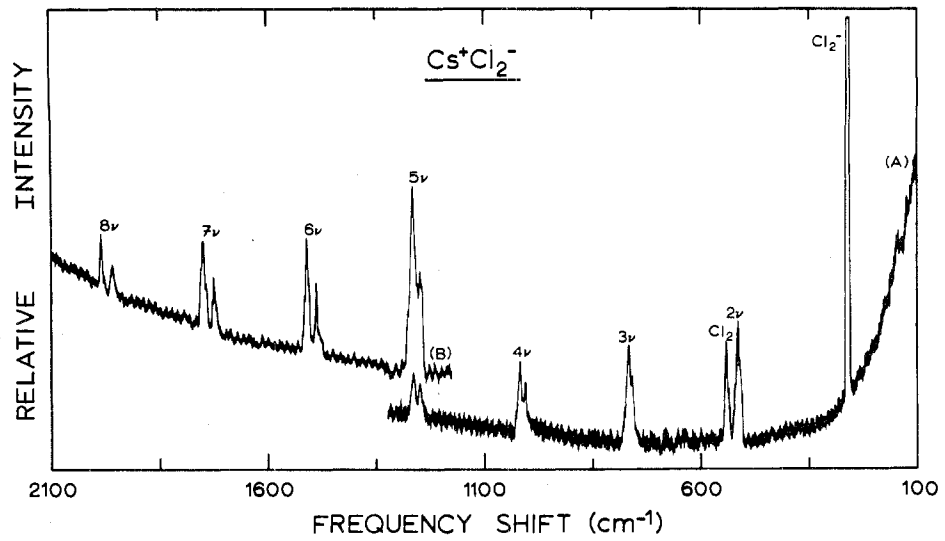

Figure 3. Resonance Raman spectrum of matrix-trapped $Cs^+Cl_2^-$. Note the $^{35}Cl^{37}Cl^-$ isotopic partners. Parameters: 75 mW of 4579-Å excitation with 12-Å dielectric filter, 20-cm^{-1}/min scan speed; (A) 0.3×10^{-9} A range, 3-sec rise time; (B) 0.1×10^{-9} A range, 10-sec rise time.

Table II. Observed and Calculated Frequencies in the Resonance Raman Progressions of $Cs^+(^{35}Cl_2)^-$ and $Cs^+(^{35}Cl^{37}Cl)^-$

Vibrational quantum no.	$Cs^+(^{35}Cl_2)^-$ freq, cm^{-1}		$Cs^+(^{35}Cl^{37}Cl)^-$ freq, cm^{-1}	
	Obsd	Calcd	Obsd	Calcd
1	259.0 ± 0.8	259.0		255.9
2	515.0 ± 0.9	515.0	508.4 ± 1.0	508.7
3	767.8 ± 0.8	767.8	758.4 ± 0.8	758.4
4	1017.8 ± 0.8	1017.6	1005.7 ± 0.8	1005.1
5	1264.2 ± 0.5	1264.3	1249.3 ± 0.6	1248.6
6	1508.1 ± 0.5	1507.8	1489.1 ± 1.1	1489.1
7	1749.3 ± 1.1	1748.3	1726.2 ± 0.7	1726.4
8	1984.5 ± 1.0	1985.7	1960.0 ± 1.2	1960.7

Raman progression in Rb–Cl_2 experiments; an intense fundamental at 260.1 ± 0.7 cm^{-1} was followed by overtones at 517.1, 771.6, 1020.2, and 1266.6 ± 1.0 cm^{-1} in a regularly decreasing pattern. Weaker counterparts were observed at 510.7, 761.5, and 1009.8 ± 1.0 cm^{-1}, and the Cl_2 feature was present at 539 and 531 cm^{-1}. Other exciting lines (4579, 5145 Å) gave shorter series.

Cesium. The most prolific set of bands found in this series of alkali metal–chlorine trials was noted with Cs. Although this family, originating at 259.0 ± 0.8 cm^{-1}, had only eight members, every signal had an observed lower frequency-shifted partner except for the fundamental. These positions are recorded in Table II, and the spectrum is reproduced in Figure 3. The two progressions were of regularly decreasing intensity and were most extensive with 4579-Å excitation. Longer wavelength laser exciting lines gave shorter series and weaker signals, as is illustrated in Figure 4.

Experiments with Cs and $^{37}Cl_2$ (99% enriched) yielded four members of the set corresponding to the families seen with natural-abundance Cl_2. A strong fundamental was calibrated at 251.3 ± 0.6 cm^{-1}, followed by regularly decreasing intensity signals at 502.2 ± 0.5, 746.5 ± 1.0, and 992.8 ± 0.5 cm^{-1}. A moderately intense $^{37}Cl_2$ feature was observed at 522.2 ± 0.5 cm^{-1}.

Barium. One experiment was done with barium metal in the Knudsen cell heated to 590 ± 5°. The resulting product band at 254 ± 1 cm^{-1} was weaker than the alkali metal counterparts.

Discussion

The isotopic Cl_2 Raman signals in the region 540–520 cm^{-1} were in excellent agreement with spectra obtained from chlorine crystals held at cryogenic temperatures[9,10] but were shifted some 16 cm^{-1} from gas-phase frequencies.[11] The agreement between the present Cl_2 matrix signal and solid measurements suggested that the bands observed in these studies were due to a vibration of aggregated Cl_2, in harmony with I_2 dilution experiments.[12] The Cl_2 crystal study of Anderson and Sun[10] assigned the triplet to isotopic splittings in the totally symmetric vibration of the D_{2h} unit cell (Cl_2

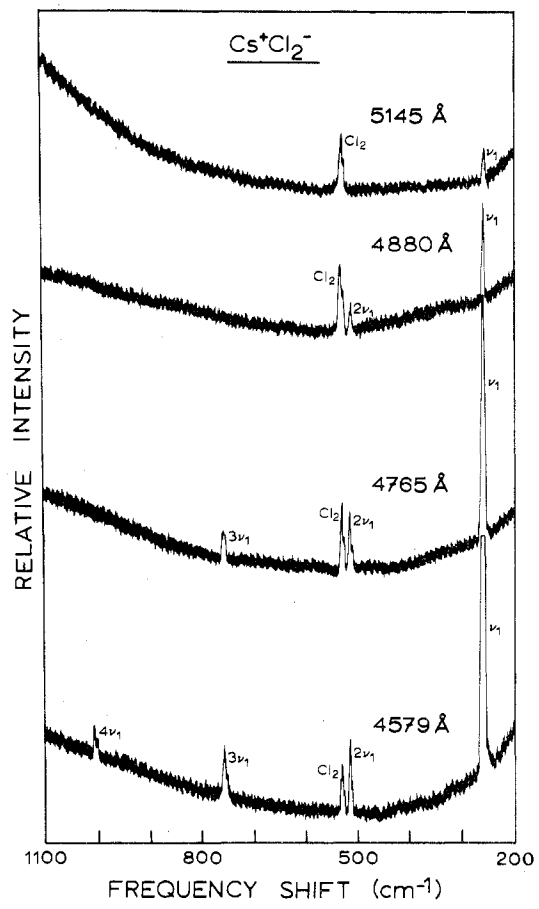

Figure 4. Wavelength dependence of laser excitation on resonance Raman spectra of matrix-isolated $Cs^+Cl_2^-$. Parameters: 20-cm^{-1}/min scan speed, 3-sec rise time, 0.1×10^{-9} A range, 5-Å dielectric filter (12 Å with 4579 Å). Laser power at sample: 5145 and 4880 Å, 150 mW; 4765 Å, 100 mW; 4579 Å, 75 mW.

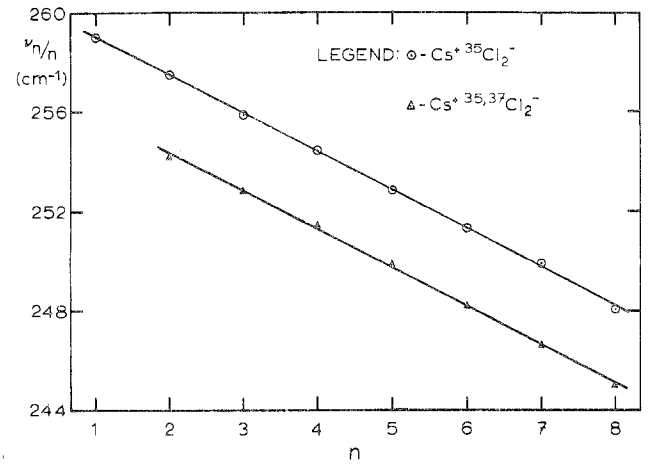

Figure 5. Plot of $\nu(n)/n$ *vs.* n (n is vibrational quantum number) for matrix-isolated $Cs^+Cl_2^-$ Raman progressions. Band calibrations accomplished with 4579-Å excitation.

dimer). Cl_2 dimer and higher aggregates are present in clusters formed during matrix sample condensation. Although this trio was quite intense, no Cl_2 overtones were observed with any Ar^+ laser line excitation. The Cl_2 signal was likely benefited by preresonance enhancement, as the absorption curve of Cl_2 reaches a maximum near 3300 Å in the ultraviolet and extends to nearly 5000 Å.[13]

Cl_2^- molecular ions in irradiated KCl exhibit an optical absorption which peaks near 3650 Å and tails out to 5000 Å;[14] the yellowish orange to reddish orange color of matrices containing alkali metal atom and chlorine reagents suggest the formation of Cl_2^- by reaction 1. The sample color denotes

$$M + Cl_2 \rightarrow M^+Cl_2^- \quad (1)$$

an absorption in the argon ion laser wavelength region, and resonance enhancement was found in the Raman spectra which contained extensive overtone series. The regularly decreasing intensity pattern in the overtone progression and the laser wavelength dependence of fundamental and overtone intensities (Figure 4 for $Cs^+Cl_2^-$) are characteristic of resonance Raman spectra.[11,15] The appreciable intensity enhancement using argon plasma blue-green excitation, as well as the sample color, suggest an absorption maximum for the chlorine molecular anion in the $M^+Cl_2^-$ species near 4500 Å, somewhat red-shifted from the Cl_2^- band in irradiated KCl.[14]

Frequency shifts of the bands in each series were subjected to statistical analysis. The well-known equation

$$\nu(n) = \omega_e n + \omega_e X_e(n^2 + n) \quad (2)$$

given by Herzberg[13] is commonly used to calculate energy levels for diatomic anharmonic oscillators. Rearrangement of eq 2 led to

$$\nu(n)/n = \omega_e + \omega_e X_e(n + 1) \quad (3)$$

$$= (\omega_e + \omega_e X_e) + \omega_e X_e(n) \quad (4)$$

which can be plotted as $\nu(n)/n$ *vs.* n, where n is the vibrational quantum number;[15] appropriate graphs were constructed for $Li^+Cl_2^-$, $Rb^+Cl_2^-$, and $Cs^+Cl_2^-$, the last of which is depicted in Figure 5. This yielded ω_e, the harmonic frequency, by extrapolation, and the slope equaled $\omega_e X_e$, the first-order anharmonic frequency. The harmonic and anharmonic vibrational constants provided a basis for the calculation of the bond dissociation energy from the expression

$$D_e = \omega_e^2/4\omega_e X_e \quad (5)$$

Dissociation energies calculated in this manner were upper limits to the actual value.

Spectroscopic constants computed from the linear plots are presented in Table III. Also note that Tables I and II offer comparisons between observed frequencies and values calculated from experimental determinations of ω_e and $\omega_e X_e$; the maximum difference between observed and calculated frequencies was only 1.3 cm^{-1}, and the average discrepancy was less than 0.7 cm^{-1}. Harmonic vibrational frequencies of isotopic partners have a theoretical ratio inversely proportional to the square root of their reduced masses; thus, appropriate treatment of $^{35}Cl_2^-$ harmonic fundamentals yielded values of 245.7 and 258.5 cm^{-1} for $Li^+(^{35}Cl^{37}Cl)^-$ and $Cs^+(^{35}Cl^{37}Cl)^-$, respectively. The agreement with the values in Table III was most gratifying. Similar calculations involving $\omega_e X_e$, which theoretically varies inversely with the reduced isotopic masses,[13] resulted in poorer correspondence, although the error limits of the experimental values were great enough to encompass the calculated constants.

Table III. Spectroscopic Constants of Some $M^+Cl_2^-$ Species As Calculated from Linear Least-Squares Plots

Molecule	ω_e, cm^{-1}	$\omega_e X_e$, cm^{-1}	D_e, eV
$Li^+(^{35}Cl_2)^-$	249.1 ± 0.3	1.61 ± 0.08	1.19 ± 0.06
$Li^+(^{35}Cl^{37}Cl)^-$	246.0 ± 0.5	1.53 ± 0.10	1.22 ± 0.08
$Rb^+(^{35}Cl_2)^-$	263.7 ± 0.6	1.71 ± 0.12	1.26 ± 0.09
$Cs^+(^{35}Cl_2)^-$	262.1 ± 0.3	1.55 ± 0.07	1.38 ± 0.06
$Cs^+(^{35}Cl^{37}Cl)^-$	259.0 ± 0.4	1.54 ± 0.09	1.35 ± 0.08

The dissociation energy of Cl_2^- is dependent on the accompanying cation, and the larger Cs^+ appeared to offer more stability to the anion than did the smaller Li^+ (*cf.* Table III). This was in keeping with studies done on Cl_3^-, where large cations [$N(C_3H_7)_4^+$, for example] were necessary to prepare the salt.[16] Person[4] has estimated the dissociation energy of Cl_2^- at 1.2 ± 0.5 eV, in close agreement with the spectroscopic values presented here. A thermodynamic route was also used to evaluate D_e; this is summarized in reactions 6–9. The

$$Cl_2^- \rightarrow Cl_2 + e^- \quad 2.38 \pm 0.1 \text{ eV}[17] \quad (6)$$

$$Cl_2 \rightarrow 2Cl \quad 2.48 \pm 0.01 \text{ eV}[18] \quad (7)$$

$$Cl + e^- \rightarrow Cl^- \quad -3.613 \pm 0.003 \text{ eV}[19] \quad (8)$$

$$Cl_2^- \rightarrow Cl + Cl^- \quad 1.25 \pm 0.11 \text{ eV} \quad (9)$$

calculated energy of eq 9 is matched by the listings in Table III within experimental errors, although the tabulated energies represent an upper limit. The average D_e for Cl_2^-, 1.28 ± 0.10 eV, predicts an electron affinity of 2.41 ± 0.1 eV for Cl_2 which is well within the error limits for the literature value.[17] The present dissociation energy calculations confirm this measure of the electron affinity of Cl_2.

The shorter series observed when Kr and Xe hosts were employed are indicative of the smaller range of diffusion and lower reaction yield in these matrices. Often Raman signals from the heavier, more scattering matrices are weaker, although the molecular chlorine triplet resolution was enhanced. The 253-cm^{-1} signal noted in Xe–Cl_2 trials has been attributed to $XeCl_2$, produced by laser photolysis.[20]

The electron transferred from the alkali metal to the Cl_2 molecule occupied an antibonding orbital, thus dropping the net bond order from 1 to 1/2. A rough approximation of the vibrational frequency of Cl_2^- on this basis would be about half that of Cl_2, and it was gratifying to note the good experimental agreement on this point.

There are two possible assignments to the Raman band found between 270 and 275 cm^{-1} (especially strong in the Na experiment): this signal may have originated from either Cl_3^- or the Cl_3 radical. Evans and Lo[16] have measured the symmetric stretching vibration of Cl_3^- salts with various cations in solution and obtained an average frequency of 268 cm^{-1}. However, the antisymmetric stretching frequency, found at approximately 240 cm^{-1} and being strongest in the infrared region,[16] was not noted in either the Li– or Na–Cl_2 infrared

Table IV. Vibrational Assignments to the Intraionic (ν_1) and Interionic (ν_2) Symmetric modes of $M^+Cl_2^-$ Which Is Assumed To Have the Triangular Geometry

Molecule	ν_1, cm^{-1}	ν_2, cm^{-1}	Molecule	ν_1, cm^{-1}	ν_2, cm^{-1}
$^6Li^+Cl_2^-$	246	552	$K^+Cl_2^-$	264	(200)[a]
$^7Li^+Cl_2^-$	246	518	$Rb^+Cl_2^-$	260	(160)[a]
$Na^+Cl_2^-$	225	(270)[a]	$Cs^+Cl_2^-$	259	(140)[a]

[a] Estimated frequencies.

trials. Nelson and Pimentel[21] have obtained a structured infrared band from Kr–Cl_2 microwave discharge-matrix studies at 374 cm^{-1}, which was assigned to the antisymmetric stretch of the Cl_3 radical. The band observed at 374 cm^{-1} in Na experiments had the same band shape and vibrational frequency as the above-mentioned signal.

Reactions appropriate to Cl_3^- and Cl_3 radical formation during sample deposition are given in eq 10–12. In order to

$$Na + Cl_2 \rightarrow NaCl + Cl \quad (10)$$

$$Cl_2 + Cl \rightarrow Cl_3 \quad (11)$$

$$Na^+Cl^- + Cl_2 \rightarrow Na^+Cl_3^- \quad (12)$$

test the mechanism suggested by (12), additional studies are in progress in this laboratory reacting alkali chloride molecules with chlorine.[25] An experiment codepositing NaCl and Cl_2 produced a very intense band at 374 cm^{-1} which identifies this absorber as $Na^+Cl_3^-$ and necessitates a reassignment of the microwave discharge product[21] as the trichloride anion. The infrared observation of $Na^+Cl_3^-$ in these experiments, the agreement with the known position of ν_1 of Cl_3^-, and the expected greater Raman intensity for Cl_3^- as compared to that for the Cl_3 radical suggest that the 274-cm^{-1} Raman signal arises from ν_1 of Cl_3^- in the $Na^+Cl_3^-$ species.

Infrared surveys of Li– and Na–Cl_2 reaction products were undertaken in a search for ν_2, the interionic stretch of $M^+Cl_2^-$. The position of the Raman ν_1 fundamental was dependent on this vibration, due to the fact that vibrational frequencies of the same symmetry repel each other. The vibrational assignments to the ν_1 modes of the $M^+Cl_2^-$ species listed in Table IV show that the $Na^+Cl_2^-$ frequency at 225 cm^{-1} is 20–30 cm^{-1} lower than the Cl_2^- modes for the other $M^+Cl_2^-$ molecules. This indicates that ν_2 of $Na^+Cl_2^-$ occurs just above 225 cm^{-1} and that mode mixing has forced ν_1 *down* and ν_2 *up* in wave numbers. Note also that ν_1 of $K^+Cl_2^-$ appears at the highest observed wave number which arises from interaction with ν_2 of $K^+Cl_2^-$ expected near 200 cm^{-1}, just below the 249-cm^{-1} absorption of matrix-isolated KCl monomer.[7] The ν_2 modes of $Rb^+Cl_2^-$ and $Cs^+Cl_2^-$ are expected at progressively lower wave numbers,[22] removing interaction with ν_1, and the position of ν_1 falls to lower wave numbers, as Table IV indicates. Since the 200-cm^{-1} estimate for $K^+Cl_2^-$ represented the lower spectral limit of the spectrometer, infrared experiments with K, Rb, and Cs were not attempted.

Assignments for the several bands observed in Li–Cl_2 infrared trials are shown in Figure 2. The monomer, dimer, and aggregate vibrational frequencies agree with those of Schlick and Schnepp[23] and Snelson and Pitzer,[6] who studied matrix-trapped species from Knudsen cell–salt effusion. Clearly, the 617- and 580-cm^{-1} signals were due to ^{6}LiCl and ^{7}LiCl, respectively, and the asymmetry of the bands was attributed to the ^{37}Cl counterparts, which were not resolved. The triplets centered at 510 and 480 cm^{-1} were assigned to the B_{3u} vibrational modes of the ^{6}LiCl and ^{7}LiCl dimers, respectively; the presence of several bands was indicative of matrix site splitting. The 493-cm^{-1} feature in the ^{6,7}Li run was the $^6Li^7LiCl_2$ complement of the above signals. The 376- and 353-cm^{-1} bands in ^{6}Li and ^{7}Li trials, respectively, and the 1-2-1 triplet centered at 362 cm^{-1} in the ^{6,7}Li experiment were ascribed to the B_{2u} vibrational modes of the dimers. All these bands, as well as the weak LiCl polymer signals at 313 and 297 cm^{-1}, showed isotopic shifts appropriate for ^{6}Li–^{7}Li substitutions.

The bands at 552 and 518 cm^{-1} in ^{6}Li and ^{7}Li trials showed no intermediate signal in the mixed-isotopic run, which indicated a single Li atom in the molecule. Further, analogous experiments with F_2 disclosed that features appearing between the monomer and highest frequency dimer positions could be due to ν_2 of $M^+F_2^-$.[1] Therefore, the 552- and 518-cm^{-1} bands are assigned to ν_2 of $^6Li^+Cl_2^-$ and $^7Li^+Cl_2^-$, respectively.

The infrared Na–Cl_2 species were assigned by comparison to salt effusion–matrix work, and the agreement was excellent.[7] The region most likely to contain a band assignable to ν_2 of $Na^+Cl_2^-$ was dominated by the NaCl dimer band at 272 cm^{-1}.

Gas-phase frequencies of ^{6}LiCl, ^{7}LiCl, and NaCl were noted at 686.2, 643.3, and 361 ± 4 cm^{-1} respectively, by earlier workers.[22,24] The gas-to-matrix shifts of these species ranged from 10% for the Li chlorides to 7.3% for NaCl. This frequency change was typical of the large dipole–induced dipole perturbations caused by the matrix host with ionic species.

Conclusions

The resonance Raman spectra of matrix-trapped Cl_2^- in the $M^+Cl_2^-$ species were examined using 4579–5145-Å Ar^+ laser excitation. Progression frequencies for the Li^+, Rb^+, and Cs^+ species were subjected to statistical analyses, which led to calculation of ω_e, ω_eX_e, and D_e of Cl_2^-. The dissociation energy was found to be in agreement with the thermodynamic value. Matrix infrared spectra of Li– and Na–Cl_2 reaction products provided an assignment for ν_2 of $Li^+Cl_2^-$, and alkali chloride vibrational frequencies for monomers, dimers, and higher aggregates proved to be in agreement with earlier work.

Acknowledgment. The authors gratefully acknowledge financial support for this research from the National Science Foundation under Grant GP-38420X and an Alfred P. Sloan Fellowship for Lester Andrews.

Registry No. $LiCl_2$, 39356-53-1; $CsCl_2$, 39356-51-9; $RbCl_2$, 39356-55-3; $NaCl_2$, 39356-54-2; KCl_2, 39356-52-0.

References and Notes

(1) W. F. Howard, Jr., and L. Andrews, *Inorg. Chem.*, **14**, 409 (1975).
(2) T. C. Castner and W. Kanzig, *J. Phys. Chem. Solids*, **3**, 178 (1957); C. J. Delbecq, W. Hayes, and P. H. Yuster, *Phys. Rev.*, **121**, 1043 (1961); D. L. Griscom, P. C. Taylor, and P. J. Berry, *J. Chem. Phys.*, **50**, 977 (1969).
(3) M. Hass and D. L. Griscom, *J. Chem. Phys.*, **51**, 5185 (1969).
(4) W. B. Person, *J. Chem. Phys.*, **38**, 109 (1963).
(5) R. E. Minturn, S. Datz, and R. L. Becker, *J. Chem. Phys.*, **44**, 1149 (1966).
(6) A. Snelson and K. S. Pitzer, *J. Phys. Chem.*, **67**, 882 (1963).
(7) Z. K. Ismail, R. H. Hauge, and J. L. Margrave, to be published.
(8) W. F. Howard, Jr., and L. Andrews, *J. Amer. Chem. Soc.*, **95**, 2056 (1973).
(9) J. E. Cahill and G. E. Leroi, *J. Chem. Phys.*, **51**, 4514 (1969).
(10) A. Anderson and T. S. Sun, *Chem. Phys. Lett.*, **6**, 611 (1970).
(11) W. Holzer, W. F. Murphy, and H. J. Bernstein, *J. Chem. Phys.*, **52**, 399 (1970).
(12) W. F. Howard, Jr., and L. Andrews, *J. Raman Spectrosc.*, in press.
(13) G. Herzberg, "Spectra of Diatomic Molecules," 2nd ed, Van Nostrand, Princeton, N.J., 1950.
(14) C. J. Delbecq, B. Smaller, and P. H. Yuster, *Phys. Rev.*, **111**, 1235 (1958).
(15) W. Kiefer and H. J. Bernstein, *Mol. Phys.*, **23**, 835 (1972).
(16) J. C. Evans and G. Y.-S. Lo, *J. Chem. Phys.*, **44**, 3638 (1966).
(17) W. A. Chupka and J. Berkowitz, *J. Chem. Phys.*, **55**, 2724 (1971).
(18) Y. V. Rao and P. Venkateswarlu, *J. Mol. Spectrosc.*, **9**, 173 (1972).
(19) R. S. Berry and C. W. Reimann, *J. Chem. Phys.*, **38**, 1546 (1963).
(20) W. F. Howard, Jr., and L. Andrews, *J. Amer. Chem. Soc.*, in press.
(21) L. Y. Nelson and G. C. Pimentel, *J. Chem. Phys.*, **47**, 3671 (1967).
(22) S. A. Rice and W. Klemperer, *J. Chem. Phys.*, **27**, 573 (1957).
(23) S. Schlick and O. Schnepp, *J. Chem. Phys.*, **41**, 463 (1964).
(24) E. F. Pearson and W. Gordy, *Phys. Rev.*, **177**, 52 (1969).
(25) B. S. Ault and L. Andrews, to be published.